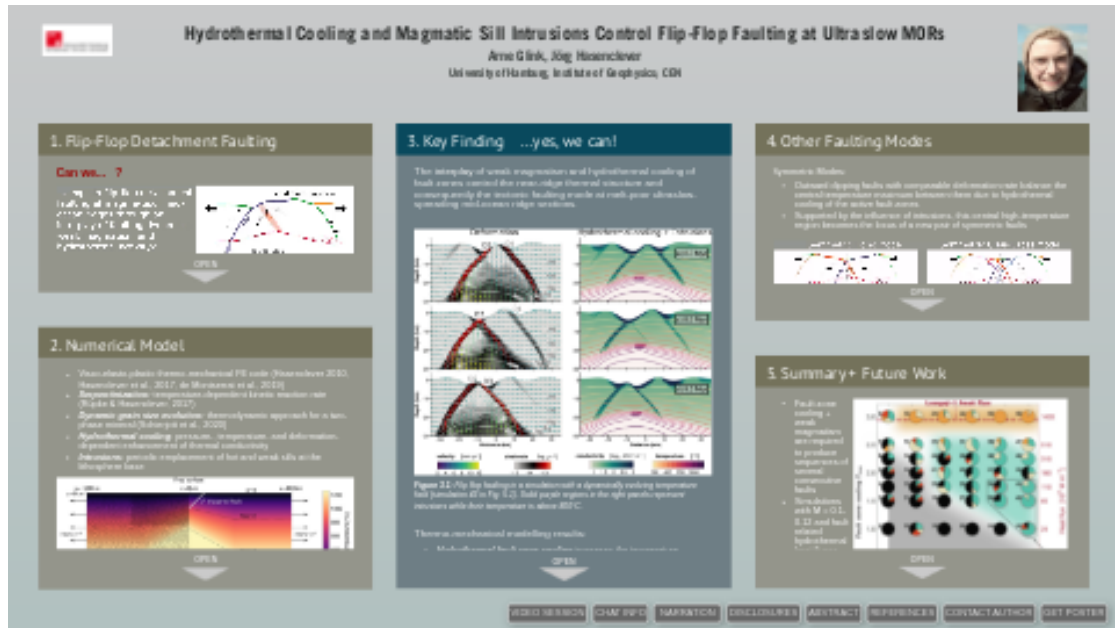


Hydrothermal Cooling and Magmatic Sill Intrusions Control Flip-Flop Faulting at Ultraslow MORs



Arne Glink, Jörg Hasenclever

University of Hamburg, Institute of Geophysics; CEN



PRESENTED AT:



1. FLIP-FLOP DETACHMENT FAULTING

Can we... ?

[VIDEO] https://res.cloudinary.com/amuze-interactive/image/upload/f_auto,q_auto/v1638861979/agu-fm2021/e8-4c-03-48-1b-25-ce-5e-7a-7b-f0-28-f2-e1-88-f6/image/sketch_ff_text_bg_t4jbk2.mp4

Figure 1.1: Sketch illustrating flip-flop dynamics.

[VIDEO] https://res.cloudinary.com/amuze-interactive/video/upload/vc_auto/v1638270053/agu-fm2021/E8-4C-03-48-1B-25-CE-5E-7A-7B-F0-28-F2-E1-88-F6/Video/steadyT_Movie_low_r9qqoq.mp4

Video 1.1: Flip flop faulting in a simulation assuming a quasi-steady thermal state. Left: strain rate and advection velocity. White lines are isotherms in 100°C increments. Top surface (sea floor) is at 4°C. Right: Grain size and serpentinization degree, isotherms in black.

The visco-elasto-plastic model simulation shown above uses a prescribed, depth-dependent temperature field similar to that by Bickert et al. (2020). Details on the model setup are given in the box below. The temperature field is only modified by the vertical displacement of the domain top representing sea floor relief. The following cycle can be observed:

1. Each new fault starts as a high-angle normal fault.
2. The footwall starts to roll back under its own weight and thereby experiences strong flexure.
3. Uplift of the footwall results in a temperature maximum in its centre. Thermal weakening in this region focusses flexural strain, which triggers grain size reduction and serpentinization, which further weakens the incipient fault zone.
4. A new fault of opposite polarity is initiated, cutting its predecessor's footwall (= flip-flop detachment fault).

Hence, a temperature maximum in the central footwall is an essential requirement to focus strain and trigger a new on-axis fault of opposite polarity.

Fault activation and stabilization is controlled by a shear localizing feedback loop between deformation, grain size reduction, and (to lower extent) serpentinization. Fig. 1.2 shows the successive strain rate increase and focusing (narrowing) of the fault. Simultaneously grain size reduces until a new detachment is initiated and becomes dominant.

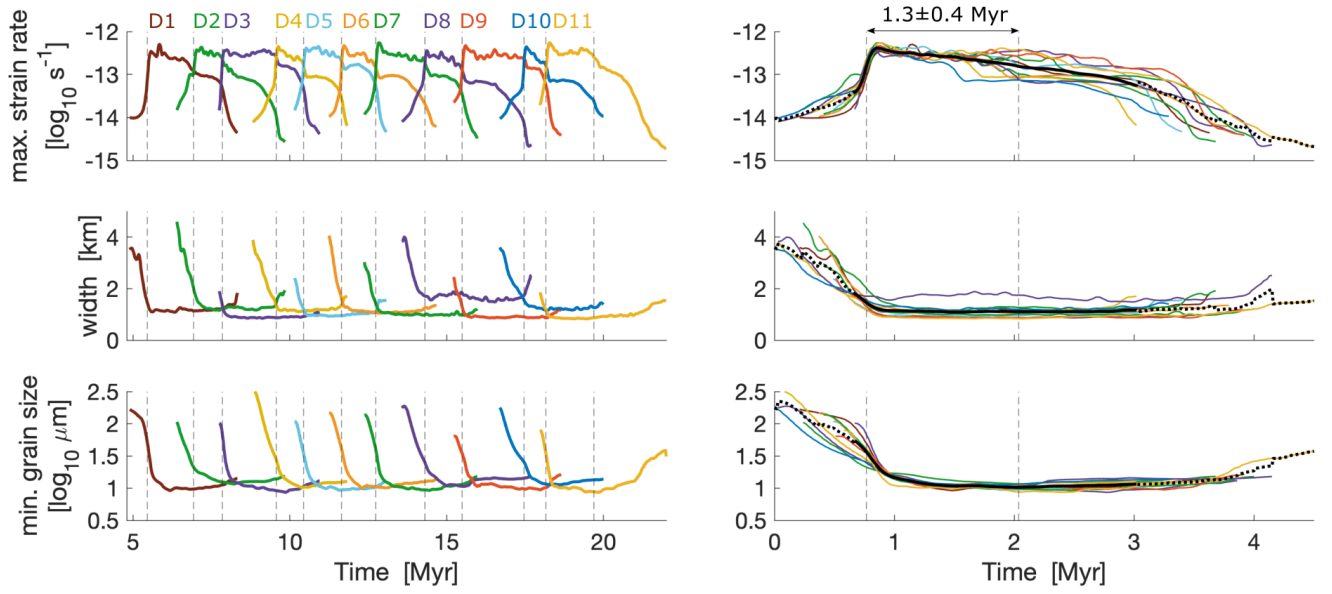


Figure 1.2: Fault zone analysis of the simulation shown above. Left: Time series of subsequent detachments after an initial adjustment phase of 5 Myr. Dashed vertical lines indicate the moment, when the strain rate of a fault exceeds that of its predecessor. Right: Same data but shifted so that the vertical lines match. The faulting cycle is very stable and fault durations match data from the South West Indian Ridge (SWIR) (1.1 ± 0.3 Myr; Cannat et al., 2019).

2. NUMERICAL MODEL

- Visco-elasto-plastic thermo-mechanical FE code (Hasenclever 2010, Hasenclever et al., 2017, de Montserrat et al., 2019)
- **Serpentinization:** temperature-dependent kinetic reaction rate (Rüpke & Hasenclever, 2017)
- **Dynamic grain size evolution:** thermodynamic approach for a two-phase mineral (Schierjott et al., 2020)
- **Hydrothermal cooling:** pressure-, temperature- and deformation-dependent enhancement of thermal conductivity
- **Intrusions:** periodic emplacement of hot and weak sills at the lithosphere base

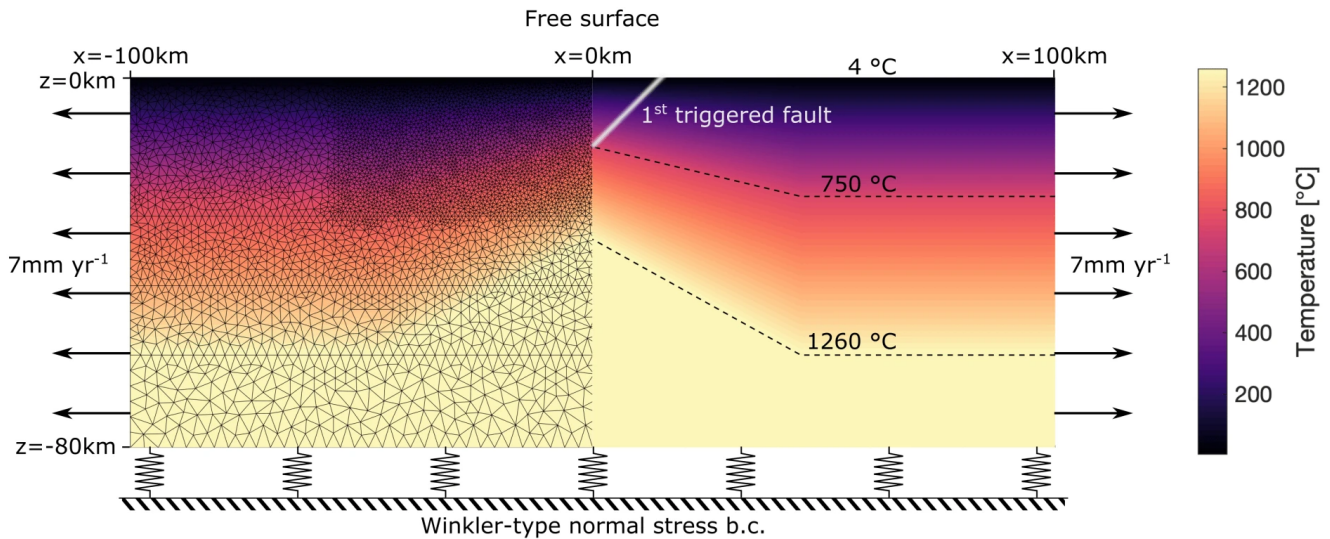


Figure 2.1: The model setup represents the setting of magma-poor segments of the SWIR at 62° E to 65° E. Shown on the left half is the triangular mesh used for the simulations. We initiate the model calculations by imposing a linear weak zone to trigger the first fault.

Important feedbacks considered by our model

Serpentinization:

Controlling factors:

- Volumetric work done by rock deformation gives a proxy for the formation of a fracture network giving water, required for the reaction, access to the rock (cf. Bickert et al., 2020)
- Thermal conditions in the serpentine stability field (< 350°C) control the reaction rate

Feedbacks on model evolution:

- Serpentine rheology is weaker than that of mantle peridotite
- Exothermic heat from the reaction

Grain size evolution:

Controlling factors:

- Ambient temperature controls grain growth as well as grain size reduction
- Grain size reduction is driven by work rate from dislocation creep

Feedbacks on model evolution:

- Diffusion creep is grain size sensitive (smaller grain size = lower viscosity)
- Grain size reduction through dynamic recrystallization consumes heat from viscous dissipation

Hydrothermal cooling:

Controlling factors:

- Hydrothermal activity (parameterized using thermal conductivity; Gregg et al., 2009) decreases with pressure and temperature (pore space closure)
- Deformation state of the lithosphere is used to enhance cooling along active fault zones (fractured rock = highly permeable fluid pathways)

Feedbacks on model evolution:

- Cooling effect on temperature field

Parameter study:

- Tested magnitudes of fault zone cooling lead to realistic heat fluxes of fault related hydrothermal fields

Magmatic sill intrusions:

Controlling factors:

- Temperature field controls emplacement below the lithosphere at the shallowest point of the basaltic solidus isotherm

Feedbacks on model evolution:

- Thermal weakening and a lower viscosity occur where partial melts are present. Rheological differences between solidified intrusions and mantle rock are disregarded for simplicity
- Latent heat from crystallization

Parameter study:

- Tested periods and sill geometries represent magmatic fractions of plate divergence (M) of 0 to 0.12

3. KEY FINDING ...YES, WE CAN!

The interplay of weak magmatism and hydrothermal cooling of fault zones control the near-ridge thermal structure and consequently the tectonic faulting mode at melt-poor ultraslow-spreading mid-ocean ridge sections.

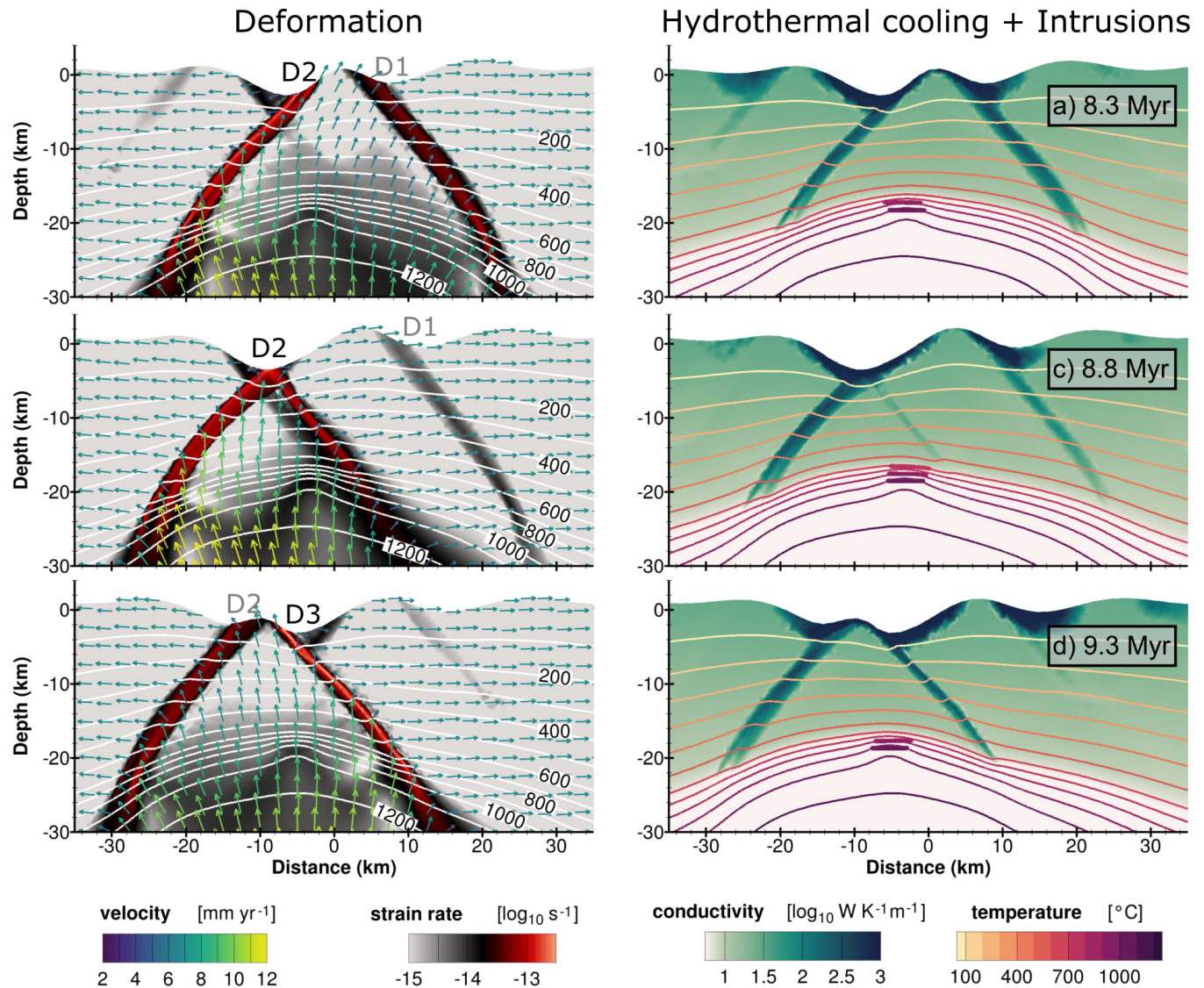


Figure 3.1: Flip flop faulting in a simulation with a dynamically evolving temperature field (simulation 43 in Fig. 5.1). Solid purple regions in the right panels represent intrusions while their temperature is above 800°C.

Thermo-mechanical modelling results:

- **Hydrothermal fault zone cooling** increases the temperature difference between the cold active detachment and its surroundings. It thereby pushes the temperature maximum caused by the upwelling hot mantle material into the footwall.

- **Intrusion emplacement** near this temperature maximum further weakens the rock and allows to focus enough strain to trigger the next fault.

[VIDEO] https://res.cloudinary.com/amuze-interactive/video/upload/vc_auto/v1638369821/agu-fm2021/E8-4C-03-48-1B-25-CE-5E-7A-7B-F0-28-F2-E1-88-F6/Video/dynT_ff_serpGSR_Movie_ppmvnk.mp4

Video 3.1: Flip flop faulting in a simulation with a dynamically evolving temperature field (simulation 43 in Fig. 5.1). Left: Strain rate & isotherms. Right: Grain size, degree of serpentinization, and black isotherms. Solid red regions represent intrusions while their temperature is above 800°C.

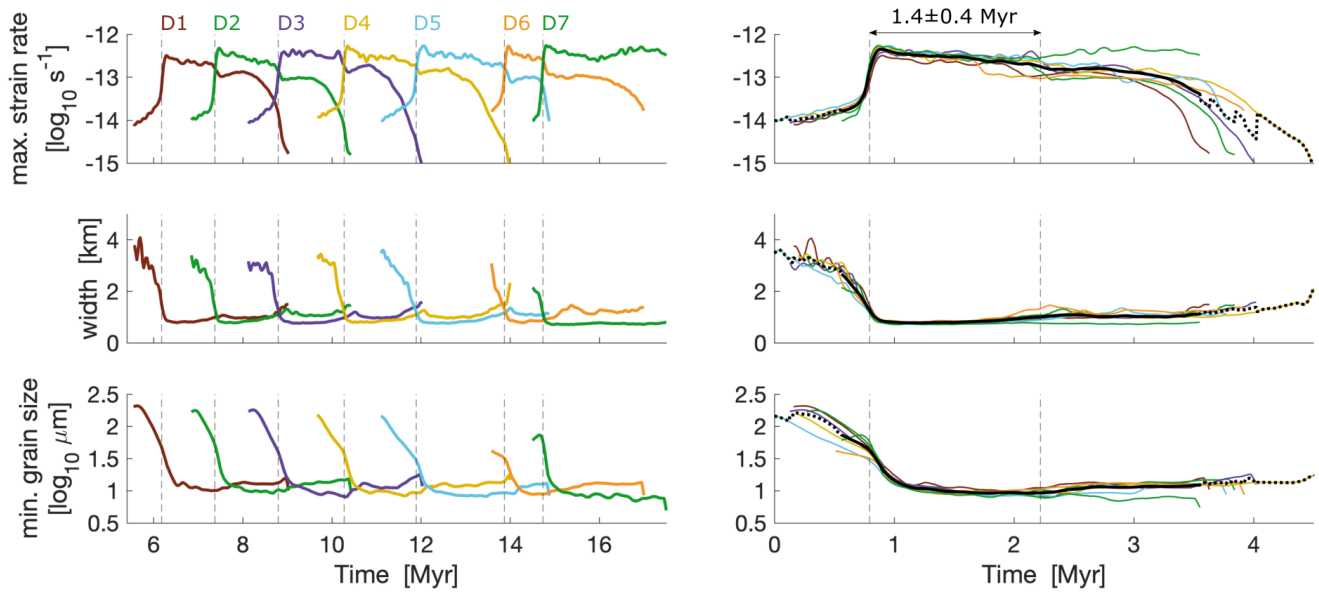


Figure 3.2: Fault zone analysis of the simulation shown above. Left: Time series of subsequent detachments after an initial adjustment phase of 5 Myr. Dashed vertical line indicate the moment, when the strain rate of a fault exceeds that of its predecessor. Right: Same data, shifted so that the vertical lines match.

Our results show that the flip-flop faulting dynamics of the thermal steady-state model (Video 1.1 and Fig. 1.2) can be reproduced with a fully dynamic thermo-mechanical model if the key processes (hydrothermal cooling and magmatic intrusions) are considered.

4. OTHER FAULTING MODES

Symmetric Modes:

- Outward dipping faults with comparable deformation rate balance the central temperature maximum between them due to hydrothermal cooling of the active fault zones
- Supported by the influence of intrusions, this central high-temperature region becomes the locus of a new pair of symmetric faults

[VIDEO] https://res.cloudinary.com/amuze-interactive/image/upload/f_auto,q_auto/v1638802093/agu-fm2021/e8-4c-03-48-1b-25-ce-5e-7a-7b-f0-28-f2-e1-88-f6/image/sketch_symm_bg_pesp2k.mp4

Figure 4.1: Sketches illustrating faulting dynamics of the two symmetric modes occurring in our thermo-mechanical model.

Symmetric Horst Mode

[VIDEO] https://res.cloudinary.com/amuze-interactive/video/upload/vc_auto/v1638368338/agu-fm2021/E8-4C-03-48-1B-25-CE-5E-7A-7B-F0-28-F2-E1-88-F6/Video/dynT_sh_serpGSR_Movie_kxfjpk.mp4

Video 4.1: Symmetric horst mode (simulation 31, Fig. 5.1). For description of the shown variables see Video 3.1 in Box 3.

- Two symmetric inward dipping shear-bands develop
- Supported by intrusion emplacements they become active faults roughly at the same time
- The enclosed central block is successively eroded while the faults migrate to their hanging wall side so that their crossing point moves upwards
- After the crossing point reaches the surface, a central horst starts to form

Symmetric Criss-Cross Mode:

[VIDEO] https://res.cloudinary.com/amuze-interactive/video/upload/vc_auto/v1638368380/agu-fm2021/E8-4C-03-48-1B-25-CE-5E-7A-7B-F0-28-F2-E1-88-F6/Video/dynT_cc_serpGSR_Movie_a5tmxz.mp4

Video 4.2: Symmetric criss-cross faulting (simulation 40, Fig. 5.1). For description of the shown variables see Video 3.1 in Box 3.

- The criss-cross mode is similar to the symmetric horst mode and occurs for calculations with stronger fault zone cooling
- Faults initiate earlier so that four faults are active at the same time
- Fault initiation is more spontaneous, presumably due to the stronger feedback between deformation and hydrothermal cooling
- The interplay of the faults at their different stages prevent the formation of a horst structure at the sea floor

Both symmetric modes create sequences of outward dipping faults, just like flip-flop faulting. Differences exist in terms of spacing (criss-cross faults are generally closer spaced), sea floor relief (criss-cross mode does not produce very pronounced ridges) and sea floor age patterns (cf. complex age pattern associated with flip-flop faulting; Cannat et al., 2019).

In contrast:

Unrealistic results without hydrothermal cooling of fault zones

[VIDEO] https://res.cloudinary.com/amuze-interactive/video/upload/vc_auto/v1638430887/agu-fm2021/E8-4C-03-48-1B-25-CE-5E-7A-7B-F0-28-F2-E1-88-F6/Video/dynT_ra_serpGSR_Movie_linkiv.mp4

Video 4.3: Long-lived detachment in a simulation without fault zone cooling and intrusions (simulation 1, Fig. 5.1). Description of the graphical framework see Video 1.1.

- Upwelling of hot mantle material close to active fault zone results in a temperature maximum at this position
- Strain in the footwall does not coincide with the position of the temperature maximum and remains unfocused
- No new fault of opposite polarity is triggered, detachments remain active unrealistically long
- Long-lived detachments are sometimes accompanied by accommodating faults of same polarity but opposite curvature (cf. beginning of the video clip)
- Temperature maximum + region of active deformation migrate away from the original position of the ridge axis, rendering this mode as unrealistic

5. SUMMARY + FUTURE WORK

- Fault zone cooling + weak magmatism are required to produce sequences of several consecutive faults
- Simulations with $M = 0.1-0.12$ and fault related hydrothermal heat fluxes about ten times that of the Lost City hydrothermal field (Lowell, 2017) yield the most stable flip-flop faulting sequences
- For stronger cooling, we observe two symmetrical faulting modes, which offer an alternative interpretation of existing sea floor data
- Along-axis variations in melt supply and faulting modes may act as stabilizing thermal and mechanical anchors; these are missing in 2-D models

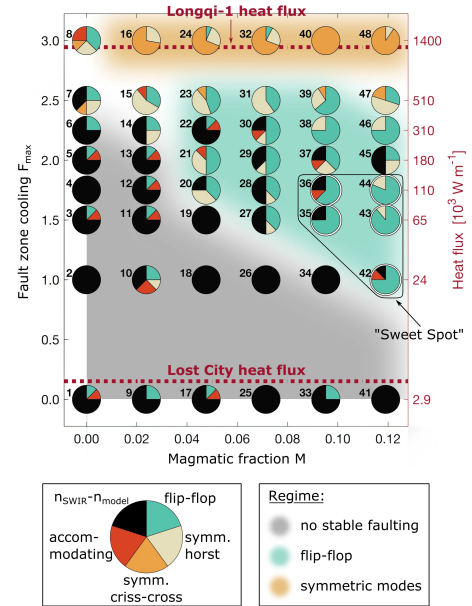


Fig. 5.1: Result of our parameter study. Pie diagrams show the different faulting modes identified in each simulation. Black slices represent the missing number of faults in comparison to the sequence of 8 consecutive detachments observed at the SWIR. Turquoise shaded area highlights the parameter region, in which flip-flop faulting dominates in our thermo-mechanical model. Literature values for the heat output of Lost City and Longqi-1 hydrothermal fields are taken from Lowell (2017) and Tao et al., (2020), respectively, divided by their fault zone parallel extent.

Open questions:

Can we use our parametrization of enhanced fault zone cooling to derive a more realistic permeability structure for hydrothermal circulation models?

- role of highly permeable fault planes: re- vs. discharge flow?
- fluid-rock interaction: feedbacks between fault initiation/stabilization and fluid circulation patterns?

DISCLOSURES

This project is funded by the German Science Foundation (DFG) through grant HO 1411/30-1, RU 1469/4-1.

ABSTRACT

Oceanic lithosphere created at mid-ocean ridges (MOR) is shaped by a complex interplay of magmatic, tectonic and hydrothermal processes. Where melt budget decreases at (ultra)slow spreading rates, the tectonic mode changes from normal to detachment faulting. We investigate an endmember type of detachment faulting, the so-called “flip-flop” detachment mode, observed exclusively at almost amagmatic sections of ultraslow-spreading MORs (e.g. Southwest Indian Ridge 62°E to 65°E): Active detachments migrate across the ridge axis towards the hanging wall side until they are superseded by a new on-axis fault of opposite polarity. Using a steady-state temperature field, numerical experiments by Bickert et al. (EPSL, 2020, 10.1016/j.epsl.2019.116048) show that an axial temperature maximum is essential to trigger flip-flop faults by focusing flexural strain in the footwall of the active fault. However, ridge segments without a significant melt budget are more likely to be in a transient thermal state controlled, at least in part, by the faulting dynamics themselves.

In our study we investigate (1) which processes have first order control on the thermal structure of the lithosphere, (2) their respective feedbacks on the mechanical evolution of the lithosphere, and (3) how they facilitate flip-flop detachment faulting. We present results of 2-D thermo-mechanical numerical modelling including serpentinization reactions and dynamic grain size evolution. The model features a novel form of parametrized hydrothermal cooling along fault zones as well as the thermal and rheological effects of periodic sill intrusions.

We find that both hydrothermal cooling of the active fault zone and periodic sill intrusions in the footwall are essential for entering the flip-flop detachment mode. Hydrothermal cooling of the fault zone pushes the temperature maximum into the footwall, while intrusions near the temperature maximum further weaken the rock and facilitate the opening of new faults with opposite polarity. We conclude that this interplay of hydrothermal cooling and magmatic intrusions is required to produce the observed flip-flop faulting. Our model allows us to put constraints on the magnitude of both processes, and we obtain reasonable melt budgets and hydrothermal heat fluxes only if both are considered.

REFERENCES

- Bickert, M., Lavier, L., Cannat, M. (2020). How do detachment faults form at ultraslow mid-ocean ridges in a thick axial lithosphere? *Earth Planet. Sci. Lett.*, 833:116048. doi:10.1016/j.epsl.2019.116048 (<https://doi.org/10.1016/j.epsl.2019.116048>).
- Cannat, M., Sauter, D., Lavier, L., Bickert, M., Momoh, E., Leroy, S. (2019). On spreading modes and magma supply at slow and ultraslow mid-ocean ridges. *Earth Planet. Sci. Lett.*, 519:223-233. doi:10.1016/j.epsl.2019.05.012 (<https://doi.org/10.1016/j.epsl.2019.05.012>).
- de Montserrat, A., Morgan, J.P., Hasenclever, J. (2019). LaCoDe: A Lagrangian two-dimensional thermo-mechanical code for large-strain compressible visco-elastic geodynamical modeling. *Tectonophysics*, 767:228173. doi:10.1016/j.tecto.2019.228173 (<https://doi.org/10.1016/j.tecto.2019.228173>).
- Gregg, P.M., Behn, M.D., Lin, J., Grove, T.L. (2009). Melt generation, crystallization, and extraction beneath segmented oceanic transform faults. *J. Geophys. Res.*, 114:B11102. doi:10.1029/2008JB006100 (<https://doi.org/10.1029/2008JB006100>).
- Hasenclever, J. (2010). *Modeling Mantle Flow and Melting Processes at Mid-Ocean Ridges and Subduction Zones - Development and Application of Numerical Models* (Doctoral dissertation, University of Hamburg, Germany). <https://ediss.sub.uni-hamburg.de/handle/ediss/3836> (<https://ediss.sub.uni-hamburg.de/handle/ediss/3836>).
- Hasenclever, J., Knorr, G., Rüpke, L.H., Kohler, P. Morgan, J.P. (2017). Sea level fall during glaciation stabilized atmospheric CO₂ by enhanced volcanic degassing. *Nat. Commun.*, 8:15867. doi:10.1038/ncomms15867 (<https://doi.org/10.1038/ncomms15867>).
- Lowell, R.P. (2017). A fault-driven circulation model for the Lost City Hydrothermal Field. *Geophys. Res. Lett.*, 44:2703-2709. doi:10.1002/2016GL072326 (<https://doi.org/10.1002/2016GL072326>).
- Rüpke, L.H., Hasenclever, J. (2017). Global rates of mantle serpentinization and H₂ production at oceanic transform faults in 3-D geodynamic model. *Geophys. Res. Lett.*, 44:6726-6734. doi:10.1002/2017GL072893 (<https://doi.org/10.1002/2017GL072893>).
- Schierjott, J.C., Thielmann, M., Rozel, A.B., Gobalek, G.J., Gerya, T.V. (2020). Can Grain Size Reduction Initiate Transform Faults? - Insights From a 3-D Numerical Study. *Tectonics*, 39:10. doi:10.1029/2019TC005793 (<https://doi.org/10.1029/2019TC005793>).
- Tao, C., Seyfried, W. E., Lowell, R. P., et al. (2020). Deep high-temperature hydrothermal circulation in a detachment faulting system on the ultra-slow spreading ridge. *Nat. Commun.*, 11:1300. doi:10.1038/s41467-020-15062-w (<https://doi.org/10.1038/s41467-020-15062-w>).

